Biosensors Based On Prussian Blue Modified Carbon Fibers Electrodes for Monitoring Lactate in The Extracellular Space of Brain Tissue

P. Salazar[1], M. Martín[1], R.D. O'Neill[2], R. Roche[1] and J.L. González-Mora[1]*

[1] Neurochemistry and Neuroimaging group, Faculty of Medicine, University of La Laguna, Tenerife, Spain.
[2] UCD School of Chemistry and Chemical Biology, University College Dublin, Belfield, Dublin 4, Ireland.
[*]E-mail: psalazar@ull.edu.es

During recent decades, a new paradigm has emerged in neuroscience from growing evidence that lactate, and not glucose, has the more important role as an energy substrate during neural activation. Based on these findings, the astrocyte–neuron–lactate shuttle hypothesis (ANLSH) has been proposed. Over the same period, biosensors have become an important tool for in-vivo studies, providing higher time and spatial resolution over microdialysis and other neuroanalytical techniques. In this work we present a new lactate microbiosensor based on Prussian Blue (PB)-modified carbon fiber electrodes (CFEs) that allows the detection of enzyme-generated hydrogen peroxide at a low applied potential (~0 V against SCE), contrasting the high overpotential used in many previous designs based on platinum transducers (~0.7 V). Here, optimization of the fabrication procedure is described, including activation of CFE/PB, enzyme immobilization, anti-biofouling and anti-interference properties. Finally, to illustrate the potential use of this approach, some in-vivo results are presented, including pharmacological, physiological and electrophysiological stimulation, showing that this microbiosensor design is well suited to exploring the role of lactate in brain extracellular fluid.

1. INTRODUCTION

During the last decade an important debate has been generated about the regulation of brain metabolic responses to neuronal activity [1-6]. Brain cells are dependent on a continuous supply of energy, glucose being its main fuel under normal physiological conditions. Because the brain has very little energy reserve, a continuous vascular supply of glucose and oxygen is mandatory to sustain

neuronal activity. Historically, lactate was considered a dead-end metabolite of glycolysis or a sign of hypoxia and anaerobic energy metabolism [7, 8]. However, a body of evidence has been accumulated to indicate that large amounts of lactate can be produced in many tissues under fully aerobic conditions [8-13]. Therefore, some authors point out that lactate could be used as a supplementary fuel [2, 14, 15], and has even been suggested to be the predominant oxidative substrate over glucose during neural activation [6, 16, 17]. Due to these findings, the astrocyte–neuron–lactate shuttle hypothesis (ANLSH) has been suggested [14, 15, 18]. According to this model, during neural activation the uptake of glutamate leads to glucose uptake into the astrocytes, and its glycolysis generates lactate which is exported into the extracellular compartment where it is taken up by neurons for its ultimate phosphorylation. This idea has divided the neuroscience community into two schools, and has generated an intense discussion [1-6, 14-22]. Most of the evidence for ANLSH are based on in-vitro experiments and on the presence of some enzymes and transporters required in the proposed hypothesis [3, 11-13]. ANLSH argues a causal sequence of events that can only be tested under in-vivo conditions. Traditionally, microdialysis has been employed for monitoring extracellular metabolites in vivo [23-25]; unfortunately, this technique often displays poor time resolution (10–30 min). More recently, biosensors have been shown to be an excellent analytical tool, providing high spatial and temporal resolution, and enough sensitivity and selectivity for in-vivo experiments [26]. In this way, microdialysis technique has been coupled with biosensor technology [27, 28], presenting as its main advance over conventional sample collection better time resolution (as low as 30 s) [29]. Nevertheless, implantable biosensors based on carbon fiber electrodes (CFEs) have smaller dimensions (~10 µm diameter) than microdialysis probes (200–500 µm), which attenuates traumatic brain injury during insertion [30], and provides yet higher time resolution, allowing real-time correlation with animal behavior [31-35].

In recent years our group has been working on Prussian Blue modified microelectrodes to detect enzyme-generated H_2O_2 at low applied potentials (0 V vs. SCE) as an alternative to conventional noble metal based transducers often employed in first-generation biosensors for physiological applications. Thanks to this approach glucose biosensors reached very low dimensions (~10 µm diameter) and displayed excellent in-vitro and in-vivo responses [32-35]. Now we present a new lactate biosensor adapting our previous glucose biosensor design, exploring and optimizing the main fabrication steps in order to improve sensitivity, stability, selectivity and anti-biofouling properties. Finally, in order to show its potential use in physiological studies we present some in-vivo experiments with this optimized lactate biosensor.

2. EXPERIMENTAL

2.1 Reagents and Solutions

The enzyme lactate oxidase (Lox) from *Pediococcus sp.*, purchased as a lyophilized powder, and glutaraldehyde (Glut, 25%) were obtained from Sigma Chemical Co., and stored at −21 ºC until use. Bovine serum albumin (BSA, fraction V) and all other chemicals, including *o*-phenylenediamine

(o-PD), lactate, polyethyleneimine (PEI), KCl, NaCl, $CaCl_2$, $FeCl_3$, $K_3[Fe(CN)_6]$, HCl (35% w/w), H_2O_2 (30% w/v), Nafion (5% w/w in a mixture of lower aliphatic alcohols and water) and phosphate buffer saline (PBS, pH 7.4 containing 0.1 M NaCl) were also obtained from Sigma, and used as supplied. The interference compounds: glucose, ascorbic acid (AA), uric acid (UA), dopamine (DA), 3,4-dihydroxyphenylacetic acid (DOPAC), serotonin (5-HT), glutamate (Glu) and glutamine (Gln) were obtained for Aldrich-Sigma, and used as supplied. PBS stock solutions were prepared in doubly distilled water (18.2 MΩ cm, Millipore-Q), and stored at 4 °C when not in use. A stock 50 mM solution of lactate was prepared in water, and stored at 4 ºC when is not in use. The PEI solutions were prepared by dissolving PEI at x% w/v in H_2O. The cross-linking solution was prepared in PBS with 1% w/v of BSA and 0.1% w/v of Glut. Monomer solution of 300 mM o-PD was prepared using 48.6 mg of o-PD and 7.5 mg of BSA in 1.5 mL of N_2 saturated PBS and sonicating for 15 min. A 100 units/mL solution of Lox was prepared by dissolving 50 units in 0.5 mL of PBS. Interference solutions were prepared in water just before use and, if necessary, the pH was adjusted to 7.4. Carbon fibers (8 μm diameter), Platinum/Iridium wire (25 μm diameter), glass capillaries, and 250 μm internal diameter Teflon-coated copper wire were obtained from Word Precision Instruments Inc. and silver epoxy paint was supplied by Sigma.

2.2 Instrumentation and Software

Experiments were computer controlled with data-acquisition software EChem™ for CV and Chart™ for constant potential amperometry (CPA). The data-acquisition system used was e-Corder 401 (EDAQ) and a low-noise and high-sensitivity potentiostat, Quadstat (EDAQ). CV and electrochemical impedance spectroscopy (EIS) experiments for micro-biosensor characterization were conducted with an Autolab PGSTAT 20 potentiostat and a FRA module from EcoChemie, computer controlled by their General Purpose Electrochemical System (GPES) and FRA software, respectively. The linear and non-linear regression analyses were performed using the graphical software package Prism (GraphPad Software, ver. 5.00). To electro-deposit and activate the PB, a custom-made Ag/AgCl/saturated KCl reference electrode and platinum wire auxiliary electrode were used.

2.3 Amperometric experiments

2.3.1 In vitro

CV and EIS experiments for PB characterization were measured in electrolyte support solution (0.1 M XCl and 0.1 M HCl (X being either Na or K)) or (0.1 M $CaCl_2$ and 0.1 M HCl). Experimental conditions for EIS measurements were: applied potential +0.1 V against SCE, signal amplitude 5 mV and frequency range 40 kHz–0.5 Hz. All in-vitro experiments were done in a 25 mL glass cell at 21 °C, using a standard three-electrode set-up with a commercial saturated calomel electrode (SCE, CRISON Instrument S.A.) as the reference and platinum wire as the auxiliary electrode. The previously determined optimum applied potential for amperometric studies on CFE/PB-based biosensors was 0 V against SCE [32-35]. Lactate calibrations were performed in quiescent air-

saturated PBS (following stabilization of the background current for 20 min) by adding aliquots of lactate stock solution to the electrochemical cell. After each addition, the solutions were stirred for 5 s and then left to reach the steady-state current.

2.3.2 In vivo

These experiments were carried out with male rats of ~300 g (Sprague Dawley) in accordance with the European Communities Council Directive of 1986 (86/609/EEC) regarding the care and use of animals for experimental procedures, and adequate measures were taken to minimize pain and discomfort. After being anesthetized with urethane (1.5 g/kg), the animal's head was immobilized in a stereotaxic frame and its body temperature maintained at 37 ºC with a heating blanket. The skull was then surgically exposed and small hole drilled for microbiosensor implantations. To measure prefrontal cortex lactate, the microbiosensor was implanted according to Paxinos and Watson coordinates: A/P +2.7 from bregma, M/L +1.2 and D/V −0.5 from dura [36]. The Ag/AgCl reference electrode and platinum auxiliary electrode were placed in the cortex, and the skull kept wet with saline-soaked pads. The reference potential provided by the Ag/AgCl wire in brain tissue is very similar to that of the SCE. For in-vivo oxygen measurement a CFE/PoPD was polarized at −0.65 V. Electrical stimulation was provided by an S-8800 Grass model and a bipolar electrode made with two unmodified CFE mounted in a two-barrel glass capillary. The exposed surface of the tip was approximately 500 µm long. Electrical stimuli parameters were: 0.15 mA of 1-ms square biphasic pulses for 3–5 seconds at 20–30 Hz. During oxygen-manipulation studies, the appropriate gas was pumped close to the rat's nose to ensure optimal exposure, and alternatively pure O_2 and N_2 were administered during ~1 min, after which the air flux was restored. Intraperitoneal injection (*i.p.*) was selected for pharmacological administration.

2.4 Preparation of the Working Electrodes

2.4.1 Fabrication of Carbon Fiber Electrodes

Carbon fibers (diameter 8 µm, 20–50 mm in length) were attached to Teflon-coated copper wire (diameter 250 µm), using high purity silver paint, and dried for 1 h at 80 ºC. The borosilicate glass capillary was pulled to a tip using a vertical microelectrode puller (Needle/Pipette puller, Model 750, David Kopf Instruments). After drying, the carbon fiber was carefully inserted into the pulled glass capillary tube under a microscope, leaving 2–4 mm of the carbon fiber protruding at the pulled end. Subsequently, the carbon fiber was cut to the desired length (approximately 250 µm) using a microsurgical scalpel. At the stem end of the capillary tube, the copper wire was fixed by casting with non-conducting epoxy glue; the carbon fiber was also sealed into the capillary mouth, using the same epoxy glue.

2.4.2 PB electro-deposition onto Carbon Fiber Electrodes

CFEs were modified by means of electro-deposition and activation of a PB film. Briefly, the PB layer was electro-deposited using CV and applying 1, 3, 6, 9 or 12 cyclic scans within the limits of –0.2 to 0.4 V at scan rate of 0.05 or 0.1 V/s in a solution containing 1.5 mM $K_3[Fe(CN)_6]$ and 1.5 mM $FeCl_3$ in 0.1 M KCl and 0.1 M HCl. These CFE/PBs were cleaned in doubly-distilled water and activated by applying another 50 cycles in electrolyte solution (0.1 M KCl and 0.1 M HCl), using the same protocol. Before being used, the CFE/PBs were cleaned again in doubly-distilled water for several seconds. Finally, the PB film was tempered for 1 h at $100 – 200\ ^oC$.

2.4.3 Micro-biosensor construction based on CFE/PB

When CFE/PBs were ready to use, the next step was to immobilize the Lox using the following protocol: 15 fast immersions in the PEI (2.5% w/v; default configuration) solution and a drying period (default 5 min at room temperature); 30 fast immersions in the Lox solution; and 15 fast immersions in the cross-linking solution (BSA/Glut). After the immobilization step, all biosensors were cured for 2 h at 37 °C and stored overnight at 4 °C in a refrigerator. Finally, an interference-rejection film of PoPD/BSA (PoPD for clarity, below) was electropolymerized over the biosensor. Electropolymerization of PoPD was carried out with a standard three-electrode setup; a custom-made Ag/AgCl /saturated KCl reference was used as the reference electrode and platinum wire as the auxiliary electrode. The electropolymerization was driven at a constant potential (+0.75 V) for 20–25 min. After the fabrication procedure of the biosensors was completed, they were cleaned in doubly-distilled water. When not in use, biosensors were stored in dry condition at 4 °C.

3. RESULTS AND DISCUSSION

3.1 Prussian Blue film: characterization and optimization

PB-modified microsensors were characterized using CV. Two well-defined characteristic peaks appeared with formal potentials of 0.1 V and 0.9 V, in good agreement with previous data [32-34, 37]. The PB ↔ PW (Prussian White) transition (Figure 1a) showed a broad composite anodic peak and narrower cathodic peak characteristic of PB redox behavior displaying a mono-electronic quasi-reversible inter-conversion ($\Delta E \sim 65$ mV and $I_{rd}/I_{ox} \sim 0.8$ at a scan rate 25 mV s^{-1}).

A clear change in the CV of PB (Figure 1a) was observed in the presence of H_2O_2: an enhancement of the cathodic current and a concomitant decrease in the anodic current. This observation reflects the catalytic reduction reaction, which can be ascribed to the reduction of H_2O_2 to water by PW, as previously reported [32, 38].

The thickness of the film, *d*, was estimated taking account of the number of unit cells present on the electrode surface, geometrical parameters of the PB cell, and the working electrode area [39], according to equation 1:

$$d = (Q_{ox}/nFA)\,(l^3 N_A/4) \qquad (1)$$

where Q_{ox} is the electrical charge associated to the anodic peak, n the number of electrons in the redox process (l), F the Faraday constant, A the electrode area (6.33×10^{-5} cm^2), l is the length of the unit cell (1.02 nm) [37] and N_A is Avogadro's number. The value 4 appears in the equation since there are four effective iron atoms in the unit cell.
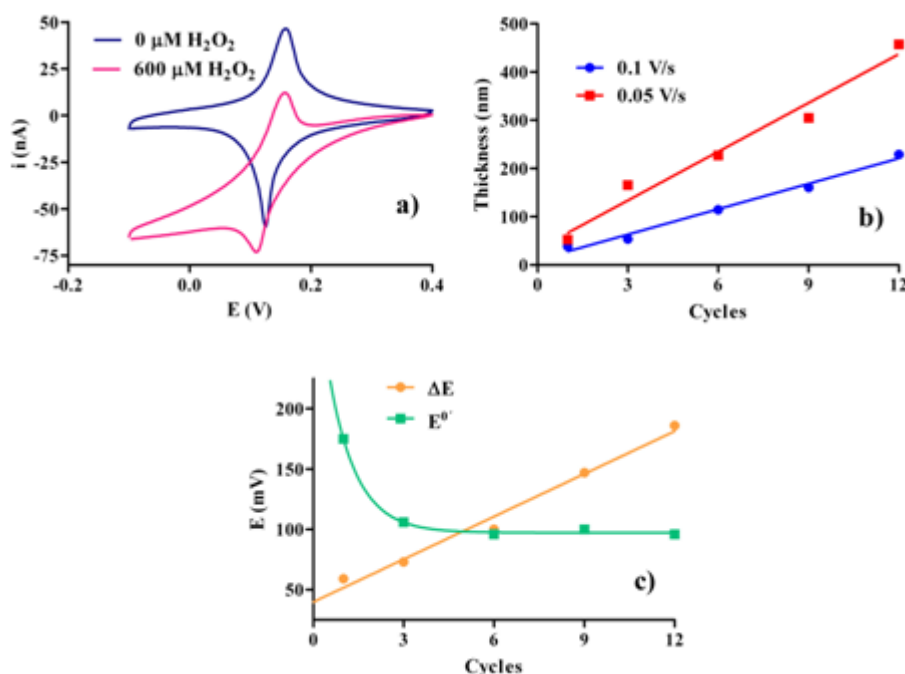

Figure 1. (a) CV for PB-modified carbon fiber electrodes (CFE/PB) without and with 600 μM H$_2$O$_2$. (b) Thickness evolution of PB deposit against the number of cycles employed during electro-deposition at two different scan rates. (c) Evolution of the peak separation (ΔE) and the formal potential (E°′) against the number of cycles applied during the electro-deposition at 0.01 V s^{-1}.

Our results indicate a linear relationship between film thickness (Figure 1b) and the number of cycles, as well as faster growth when the potential scan rate was decreased (*i.e.*, 17 and 35 nm/cycle at 0.1 and 0.05 V s^{-1}, respectively), in agreement with previous reports [40]. The PB film deposited at 0.1 V s^{-1} showed a positive correlation between peak separation, ΔE, and the number of cycles (Figure 1c). In contrast, the formal potential, $E^{0\prime}$, remained constant after 3 cycles (Figure 1c). From these results, 0.1 V s^{-1} and three cycles were selected to deposit a thin film onto CFEs for biosensor fabrication (*Section 3.2*), which gave a thickness of 51 ± 5 nm (mean ± SD, $n = 6$).

The CV shape of deposited PB films showed a clear dependence on the ionic composition of the background electrolyte solution (Figure 2, inset). Previously, it has been demonstrated that PB films display a specific transport of alkali metal cations due to its zeolite structure [32, 37]. These geometrical conditions affect the transport of cations during PB ↔ PW transitions, determining its electrochemical properties. In order to explore the ionic transport across the film, electrochemical

impedance spectroscopy (EIS) was used. EIS is an effective method to probe the interfacial properties of surface-modified electrodes [39, 41, 42]. The experimental Faradaic impedance spectra were fitted using a general Randles electronic equivalent circuit (for details see reference [34]), which is very often used to model interfacial phenomena [42]. The semicircle diameter in the impedance spectrum (Figure 2), equates to the charge-transfer resistance, R_{ct}, and displays a clear dependence on cation diffusion.
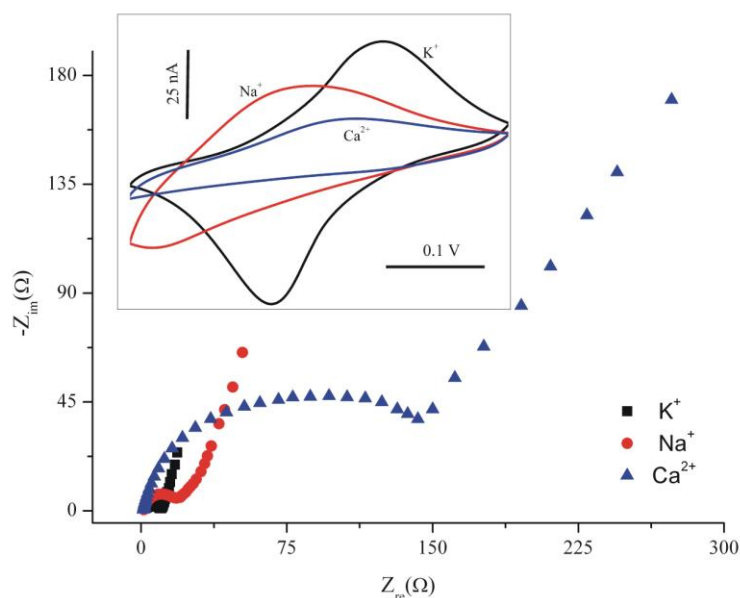

Figure 2. EIS of PB-modified carbon fiber electrodes (CFE/PB) in different background electrolytes: 0.1 M KCl, NaCl or CaCl₂, with 0.02 M HCl. Stabilization potential: +0.1 V vs. SCE, signal amplitude: 5 mV and frequency range: 40 kHz−0.5 Hz. Inset: CV of PB-modified carbon fiber electrodes (CFE/PB) in different background electrolytes: 0.1 M KCl, NaCl or CaCl₂, with 0.02 M HCl, scan rate 0.1 V s⁻¹ vs. SCE.

Our results showed that more highly hydrated cations (Ca^{2+}) display higher R_{ct}, whereas lesser hydrated cations, with lower resistance values ($K^+ < Na^+$), exhibits facilitated transport across the film, consistent with the CV shapes shown in Figure 2 (inset).

Freshly deposited PB films have been shown to be highly hydrated and unstable; accordingly, some authors have suggested activation and heat-treatment steps before their use [43, 44]. In our case activation was carried out in electrolyte solution (0.1 M HCl, 0.1 M KCl), using the same parameters as in the deposition step until the CV was stable (~50 cycles). Heat treatment was then investigated at different temperatures for 1 hour, and its effect on PB electro-chromic properties studied. The CVs for PB (Figure 3a) after heat treatment showed a progressive peak-current decrease and a significant lost of electrochemical activity at 200 ºC. The FTIR and UV-Vis absorbance spectra of the as-deposited PB film showed the characteristic Fe–CN band (2067 cm⁻¹) related to the stretching vibration of Fe–CN and the broad absorption peak at 672 nm due to charge transfer between Fe^{3+} to Fe^{2+} ions, respectively [32]. The FTIR spectrum (Figure 3b) in the high frequency region was characterized by a very broad band which can be attributed to stretching modes of bonded (2973 cm⁻¹) and free (3435 cm⁻¹) OH

groups of water [45, 46]. This band shows that water molecules can be found in PB, either coordinated in the shell of high spin iron or occupying interstitial positions as uncoordinated water. With heat treatment these bands gradually decrease in intensity. On the other hand, the Fe–CN band suffers only a slight decrease up to 150 $^{\circ}$C, but almost disappeared at 200 $^{\circ}$C, showing a clear thermal decomposition of PB. The UV-Vis spectrum (Figure 3c) showed a similar behavior discussed for the FTIR, although at 200 $^{\circ}$C it displayed a typical rust color and a clear band between 300 and 400 nm that corresponds to the wavelength region of Fe_2O_3 [47]. In view of these results, 100 $^{\circ}$C was selected for further investigation.

The effect of pH during electro-deposition was studied by using different electrolyte solutions: 0.02 (Figure 3d$_i$) and 0.1 M HCl (Figure 3d$_j$ and 3d$_k$), and then cycling CFE/PB at 0.1 V s^{-1} (~33 min) in PBS (pH 6). Our results indicate that PB films deposited in the more acid medium (Figure 3d$_j$) showed better stability, whereas PB electro-deposited with 0.02 M HCl (Figure 3d$_i$) showed a significant peak reduction when the first and the last (150th) cycles were compared. Nevertheless, only with an additional thermal treatment (Figure 3d$_k$), does PB display enough stability for useful application in electro-analytical devices.
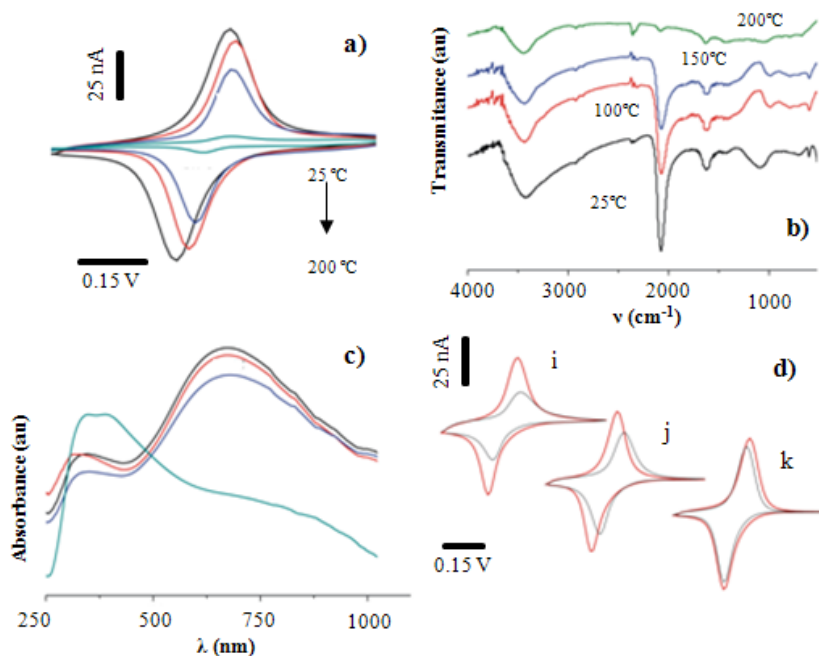

Figure 3.– Effect of annealing PB films at different temperatures, illustrated by CV (a), FTIR (b) and UV–Vis (c) spectra. (d) Stability for PB-modified electrodes (CFE/PB) electrodeposited at different pH conditions (scan-1 in *red*; scan-150 in *blue*: 0.02 M HCl (*i*) and 0.1 M HCl (*j*) and (*k*), without (*j*) and with (*k*) thermal treatment.

3.2 Lactate biosensor optimization

Following the design of glucose microbiosensors developed by our group [32-35], we assembled new lactate microbiosensors. Previously we showed that enzyme loading depends on the

number of dip-immersions employed during the manufacturing process [33]. Consequently, in the present work this number was fixed at 30 fast immersions. The first parameter investigated was the enzyme concentration. In order to optimize this concentration several biosensors were assembled using different Lox concentrations (25, 50 and 100 U mL^{-1}). Calibration curves for these biosensors (Figure 4a) showed that 100 U mL^{-1} displayed the best result with V_{max} [26] 15 times higher than the lowest concentration; for further studies this concentration was selected.
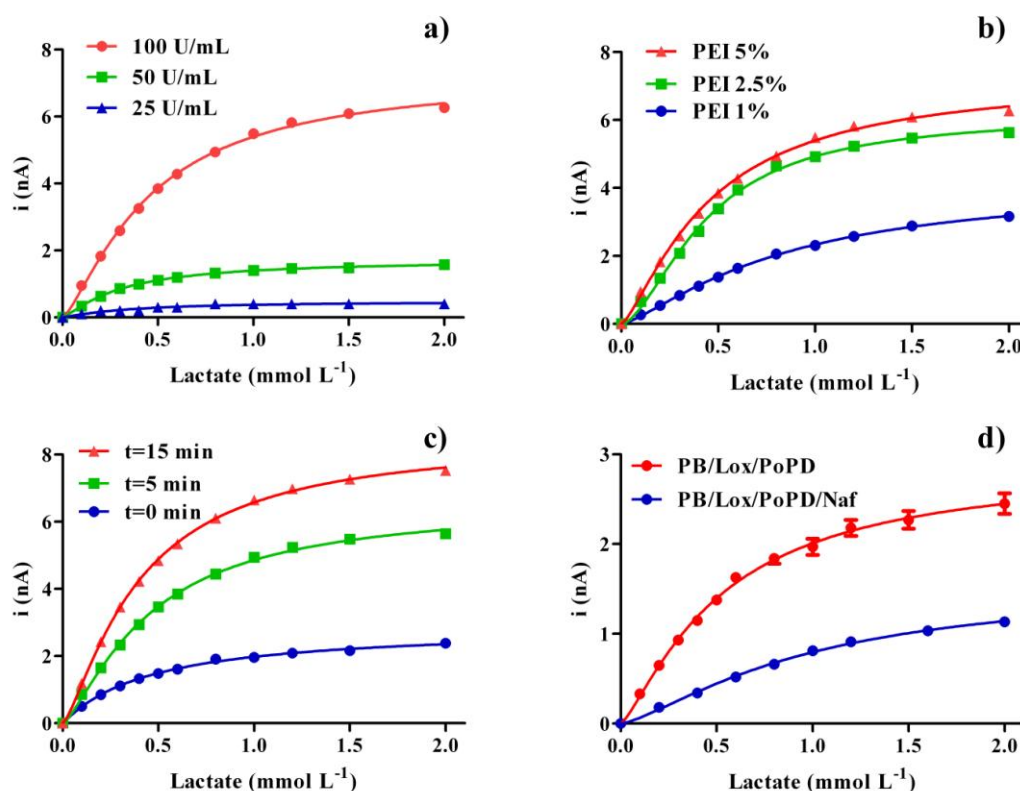

Figure 4.– Calibration curves for different lactate biosensors during optimization by changing different assembly parameters: (a) enzyme concentration, (b) polyethyleneimine (PEI) concentration, and (c) drying time between PEI immersion and enzyme loading. (d) Calibration curves for both types of lactate biosensors proposed in the present work (mean $\pm$ SEM, $n = 4$). The background electrolyte solution was PBS (0.1 M NaCl) pH 7.4; the applied potential was 0 V against SCE.

The next step was to study the effect on the enzyme loading of a polyelectrolyte such as PEI [33-34]. In recent years its ability to inhibit enzyme inactivation, and to improve its stability by the formation of cationic–anionic complexes, has been exploited [48]. In this context we studied the optimal concentration of PEI and how water content affects the enzyme loading during biosensor assembly. Responding to the first question, several PEI solutions were prepared (1, 2.5 and 5 % w/v) in water and used during biosensor construction. Figure 4b shows that both 2.5 and 5 % w/v almost doubled the enzyme loading (higher V_{max} values) compared with 1% w/v. So 2.5 % w/v PEI was maintained for further studies. Until now a drying period of 5 min was employed between immersion

in PEI and Lox solutions. In order to explore if water content affects the enzyme loading, several drying times were selected (0, 5 and 15 min). Our results (Figure 4c) suggest that longer drying times provide higher enzyme loading (V_{max} ~ 3 times with respect to the wet configuration), and that the hydration conditions of PEI are an important parameter in order to improve the enzyme loading. On the basis of these data, drying times were increased to 15 min in the following development studies.

The final step during microbiosensor construction was the addition of an external permselective film, (Lox/PoPD), which improves anti-biofouling properties and selectivity against potential endogenous interferences such as AA, UA, DA, *etc*. [32-34, 49]. First results showed a significant loss of sensitivity (~60%) that may be attributed to several factors such as: enzyme deactivation, the new diffusion barrier [32-34] and electrostatic repulsion between BSA and lactate anions. Figure 4d shows calibration data for lactate microbiosensors incorporating PoPD. Enzyme parameters, obtained using a Hill-modified Michaelis–Menten equation [50], and analytical parameters are summarized in Table 1. Lox/PoPD showed a linear range up to 0.6 mM with a sensitivity (S) of 2.68 ± 0.12 nA mM^{-1} (~42 nA µM^{-1} cm^{-2}); meanwhile the detection limit (S/N = 3) and reproducibility (CV%) were ~6 µM and 4 %, respectively.

Taking into account that extracellular fluid (ECF) concentration of lactate is ~0.4 mM [51, 52] and that changes registered during neuronal activation may reach ~200% of its basal concentration (~0.7 mM) [10, 51, 52], the present configuration possessed excellent sensitivity, but the operational linear range is pretty tight for use in physiological applications. However, we were able to increase the linear range up to 1.2 mM by means of an external Nafion film (Lox/PoPD/Naf). Three dip immersions in 5% Nafion proved enough for our purpose, whereas a higher number of dips (eight) resulted in the complete loss of sensitivity. This new diffusion film provides a barrier to lactate, decreasing sensitivity to 0.77 nA mM^{-1} (~12 nA µM^{-1} cm^{-2}) by both decreasing V_{max} and increasing K´ [26] (see Table 1). Meanwhile free diffusion of O_2 to the enzyme was maintained where it is needed to regenerate its active center. Thus we present two possible configurations that may be used depending on the in-vivo requirements.

Table 1. Enzyme kinetic (apparent Michaelis constant (K'), calibration plateau (V_{max}), and Hill coefficient (*h*)), and analytical parameters (sensitivity (S), coefficient of determination (R^2), detection limit (D.L.), linear range (L.R.) and coefficient of variation (CV%)) of different *optimized* lactate biosensor designs, Mean $\pm$ SEM, n = 4. D.L. was calculated as $3 \times$ SD of the background current. The Hill parameter is included to highlight possible deviations from straightforward Michaelis–Menten kinetics, for which *h* = 1. Calibration curves were obtained by applying 0 V against SCE in air-saturated PBS 0.1 M NaCl (pH 7.4).

Configuration	K' (mM)	Vmax (nA)	h	S (nA mM-1)	S (nA µM-1 cm-2)	R2	D.L. (M)	L.R. (mM)	CV (%)
PB/Lox/PoPD (n =4)	0.44 ± 0.05	2.88 ± 0.09	1.3 ± 0.1	2.68 ± 0.09	42.3 ± 1.5	0.994	$5.6 \cdot 10^{-6}$	D.L - 0.6	7.1
PB/Lox/PoPD/Naf (n =4)	0.97 ± 0.14	1.57 ± 0.1	1.4 ± 0.1	0.77 ± 0.03	12.2 ± 0.4	0.994	$16.8 \cdot 10^{-6}$	D.L - 1.2	6.7

Another two important questions, when designing sensors for an electrochemically hostile environment such as brain [53], are protein biofouling and interference response. In order to study the anti-biofouling properties of our biosensors, they (with and without PoPD/Naf) were immersed for 18 h in a solution of BSA (10% w/v), and lactate sensitivity before and after BSA exposure determined in its linear range (*n* = 3). Surprisingly, both configurations showed no significant difference (two-tailed paired *t*-test, *p*-value: 0.11 and 0.07, respectively) before and after being dipped in the protein solution, demonstrating the excellent anti-biofouling properties of the present configurations (Figure 5a). In this sense, PoPD films have been shown to be stable during long periods (~15 days) in in-vivo experiments, displaying excellent biocompatibility and anti-interference properties [26, 52].

Non-optimized lactate biosensors free of PoPD film (Figure 5b) showed good anti-interference properties (as a result of the low applied potential used to detect H_2O_2 at the PB-modified surface) for a considerable number of interference species and metabolites at their basal concentration [34], and responded well to lactate additions (c: 0.4 and g: 0.2 mM). Only AA (0.2 mM), one of the major endogenous interferences in the CNS, produced a clear change in the biosensor current, indicating that although we were working at a low potential, we needed an additional permselective film to avoid AA effects on biosensor responses [49]. Finally, the optimized lactate biosensor (with an external PoPD/Naf film) didn't response to the main interferences and metabolites (including AA; see Figure 5c).
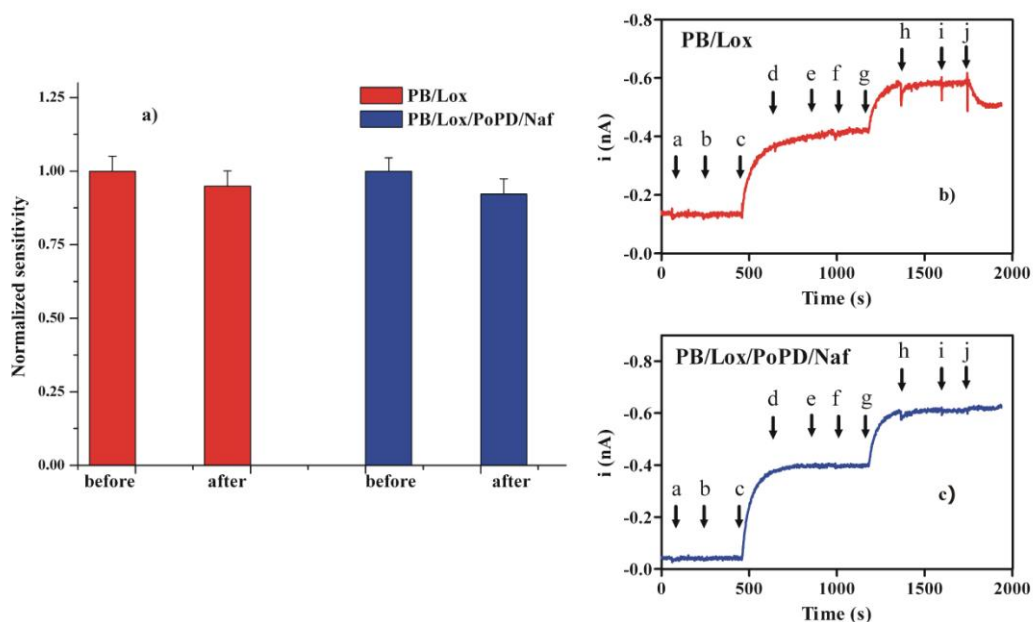

Figure 5. (a) Normalized sensitivity (mean $\pm$ SEM, *n* = 4) for PB/Lox and PB/Lox/PoPD/Naf configurations before and after being immersed in a BSA solution (10% w/v) for 18 h. Amperometric response for *non–optimized* PB/Lox (b) and *optimized* PB/Lox/PoPD/Naf (c) configurations with successive additions of: (a) 10 nM dopamine (DA), (b) 10 µM 3,4-dihydroxyphenylacetic acid (DOPAC), (c) 0.4 mM lactate, (d) 10 nM serotonin (5-HT), (e) 20 µM glutamate (Glu), (f) 0.4 mM glutamine (Gln), (g) 0.2 mM lactate, (h) 1 mM glucose, (i) 10 µM uric acid (UA) and (j) 0.2 mM ascorbic acid (AA). Calibration conditions as in Figure 4.

3.3 Lactate biosensor measurements in in-vivo experiments

Although there is an extensive bibliography about lactate biosensors [54-60], there are few papers published regarding lactate microbiosensors measuring directly in the CNS [10, 51, 52, 61, 62]. Much of these reports were based on either modified Pt transducers [10, 51], ceramic-based multisite microelectrodes [62] or CFEs [52, 61], working at a high applied potential (~0.7 V) [10, 51, 62] or using differential normal pulse voltammetry (DNPV) [52, 61] to detect the H_2O_2 generated during the enzymatic reaction. Here we present, for the first time, a lactate microbiosensor based on PB-modified CFE that is able to detect physiological changes in lactate levels at a low applied potential in the CNS.

For all in-vivo experiments, a time of 30 min after biosensor insertion was used to stabilize the baseline current. This was used to estimate the basal lactate concentration, comparing this current with previous calibration data. The basal lactate concentration (0.36 ± 0.02 mM, mean $\pm$ SD, $n = 5$) was in good agreement with previous data reported by other authors [51, 52], although factors such as the state of anesthesia will influence such comparisons [63].

It is known that extracellular fluid lactate concentration can be increased by the stimulation of neuronal activity [2, 14, 15, 52] and studies concerning such a stimulation by glutamate and *N*-methyl-D-aspartate (NMDA) have been reported [52]. In the present work, we also used NMDA, an ionotropic glutamate receptor agonist. After obtaining a stable baseline for the biosensors (normalized basal response: 100 ± 12 %; mean $\pm$ SD, n = 3), NMDA (5 mg in 2 mL PBS) was administered (*i.p.*). After 5–10 min a clear increase in lactate level was observed reaching a value of 205 ± 13 % which remained at this level for ~1 h. These results are in good concordance with previous data [52] and with ANLSH [2, 6, 14-18].

The lactate biosensor response was also evaluated during electrophysiological stimulation. In this context, local electrical stimulation was applied (30 Hz for 3 s) at intervals of 3 min approximately, allowing enough time to reach the basal resting level again. Data showed (Figure 6a) a slight decrease (~25 %) in lactate level during local electrical stimulation, suggesting that lactate is consumed during neural activity. After that, an increase in extracellular lactate concentrations (~90 % of the basal concentration) appears to be a response of the tissue to the demand for additional energy [10, 14-18]. Similar results were obtained with a lactate biosensor employing a 25-μm diameter Pt wire transducer and detecting H_2O_2 at +0.7 V (Figure 6b), the configuration commonly employed in biosensors for in-vivo applications, validating the kinetic and physiological lactate response. Finally, theses data are in good agreement with previous publications where extracellular lactate concentration fluctuations and its relationships with neural activity were explored in the dentate gyrus of the hippocampus of the rat brain after electrical stimulation of the perforant pathway [10].

The last sets of experiments were conducted to study changes of lactate and O_2 in the extracellular compartment. An O_2 sensor was constructed by coating an unmodified CFE with PoPD (CFE/PoPD) to reject interferences and to improve biocompatibility properties of the sensor [51]. This sensor was polarized at –0.65 V to detect O_2 [64]. Firstly, the in-vivo oxygen response was checked by changing extracellular oxygen concentration *via* gas administration (pure O_2 or N_2). Under these conditions, the O_2 sensor showed a clear current increase during mild hyperoxia (O_2 supply; Figure 7a), whereas the same period of mild hypoxia (N_2 supply) showed the opposite effect (Figure 7b).

Under these conditions, the O_2 signal suffered a change of 40–50% with respect to its basal level, in good agreement with previous work [65]. Changes in both cases were immediate and, on cessation of gas administration, the signals quickly returned to baseline levels indicating a rapid return to normoxic conditions. These results confirmed that CFE/PoPDs implanted in anesthetized animals respond rapidly to changes in cerebral tissue O_2 concentrations.
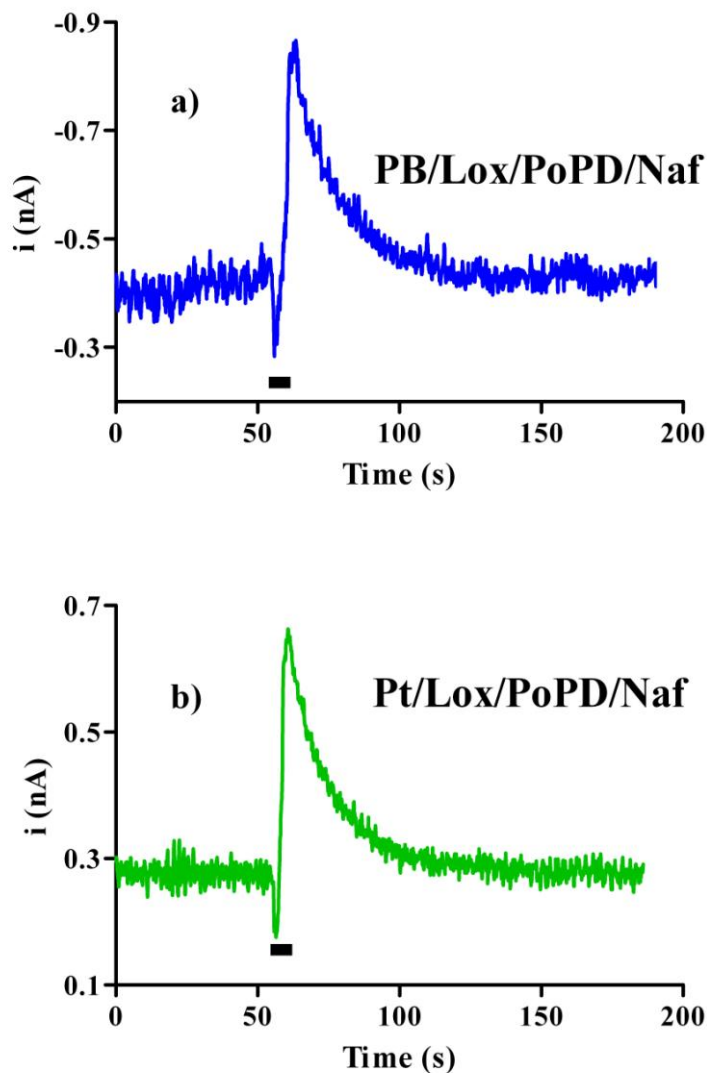

Figure 6. Extracellular lactate changes during electrical stimulation (30 Hz, 3 s) registered in the prefrontal cortex of an anesthetized rat. Data were obtained with (a) a PB/Lox/PoPD/Naf biosensor and with (b) a Pt/Lox/PoPD/Naf biosensor proposed in the present work

In order to study simultaneous changes in lactate and O_2 levels, both sensors were inserted in the prefrontal cortex close to the stimulation electrodes (50–100 μm). Electrical stimulation (20 Hz during 5 s) generated a lactate change consisting of a short period of lactate consumption followed by an increase of almost 90 % of the basal lactate concentration, similar to that seen in Figure 6 (see Figure 7c). In contrast, the O_2 sensor response showed an immediate decrease in extracellular O_2 levels (~20% of the basal value) during the stimulation, and this level was held for ~30 s after the stimulus. A

similar time was needed to reach the lactate basal level after stimulation. Taking into account that extracellular analyte concentrations are determined by a balance between consumption and supply from different compartments, these data reveal that O_2 may be consumed during oxidative processes (TCA cycles) in active neurons [1-6], and lactate could serve as an additional non-oxidative fuel during activation events [2, 14, 15] or may be the predominant oxidative substrate [6, 16, 17]. Nevertheless to obtain more robust arguments, additional experiments will be needed. At this point, these experiments have been presented to illustrate the potential use of our lactate biosensors in physiological applications. Future work will be done in order to explore lactate changes during neural activation and its relationship with hemodynamic responses, and with other metabolic substrates such as glucose, pyruvate and O_2.
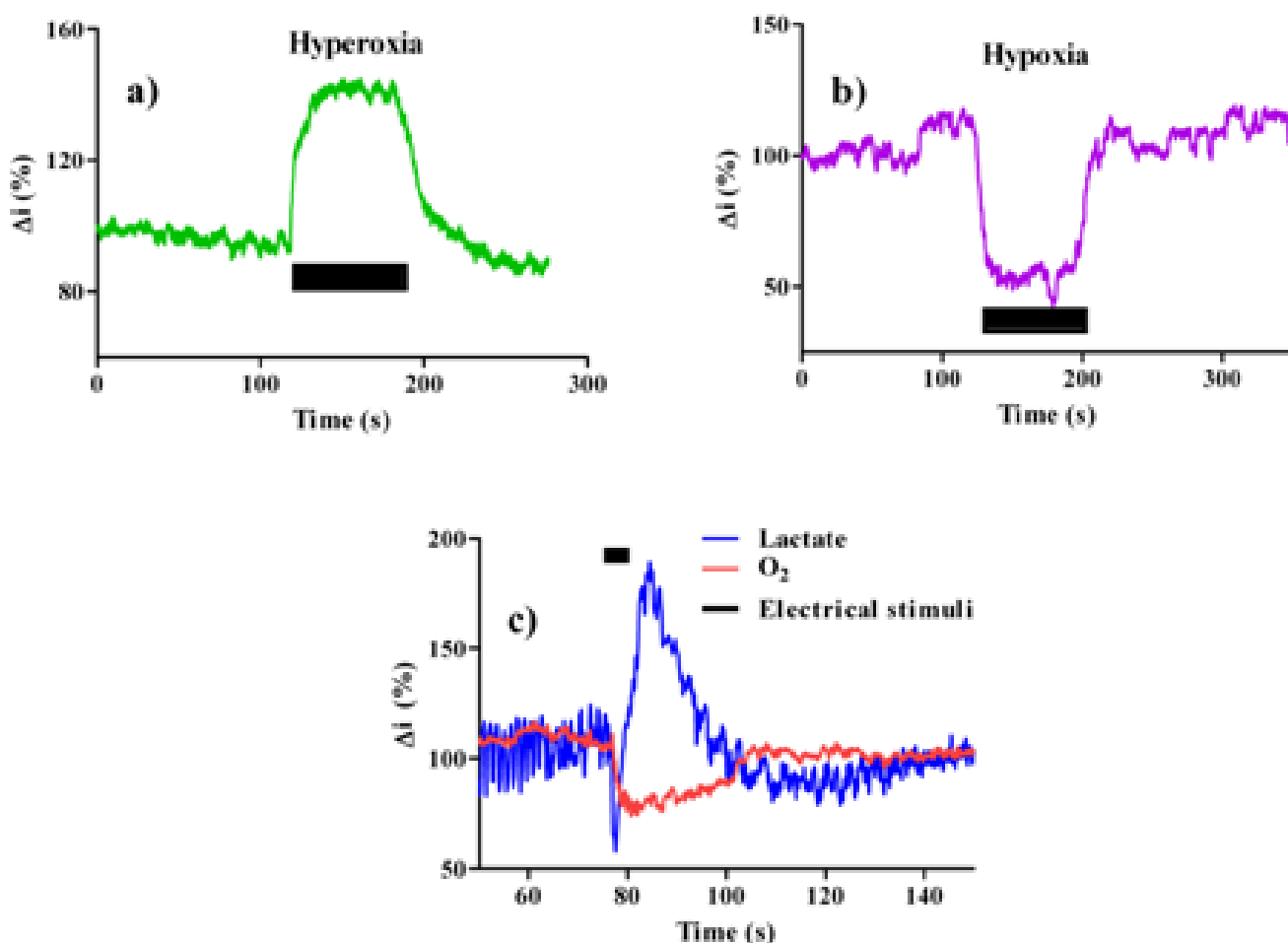

Figure 7. Effect of physiological manipulation of prefrontal cortex dissolved oxygen, monitored using a CFE/PoPD sensor. Exposing the animal briefly to pure oxygen (a), the ECF oxygen concentration promptly increased (~160% of baseline), returning back after restoration of a normal atmosphere. In contrast, exposure to nitrogen (b), induced a short-lasting decline in brain oxygen levels (~50%) which recovered promptly following nitrogen removal. (c) Simultaneous changes in lactate biosensor and oxygen (CFE/PoPD) sensor signals before, during and after electrical stimulation (20 Hz, 5 s) recorded in the prefrontal cortex of an anesthetized rat.

4. CONCLUSIONS

In this study we present a novel lactate microbiosensor based on PB-modified CFEs. This approach allows the detection of H_2O_2 enzymatically generated in the biosensor surface layer at low applied potential (0 V against SCE), instead of the high potential (+0.7 V against SCE) commonly used with the Pt transducers. During construction, each step was studied in detail in order to obtain an optimized configuration determined by functional and biocompatibility needs of neurochemical applications. In this way PB electro-deposition was studied and film properties were characterized using CV, EIS, IR and Vis-UV techniques. After optimizing the protocol to modify the CFEs with this electrocatalytic compound (PB), the next step was its modification with lactate oxidase. In this context, biosensor responses were honed to the special conditions needed for physiological applications such as: sensitivity, selectivity, operational linear range, biocompatibility, *etc*. Finally, an optimized lactate biosensor is presented and some in-vivo results shown to illustrate its application in the study of lactate and oxygen in the brain during neuronal activation.

References

1. T.M. Bliss, R.M. Sapolsky, *Brain Res.,* 899 (2001) 134
2. A. K. Bouzier–Sore, M. Merle, P.J. Magistretti, L. Pellerin, *J. Physiol. Paris* 96 (2002) 273
3. L.H. Bergersen, *Neuroscience* 145 (2007) 11
4. L. Hertz, M. Fillenz, *Neurochem. Int*. 34 (1999) 71
5. C.P. Chih, E.L. Roberts, *J. Cerebr. Blood Flow Metab*. 23 (2003) 1263
6. A.K. Bouzier–Sore, P Voisin, P Canioni, P.J. Magistretti, L. Pellerin, *J. Cerebr. Blood Flow Metab*. 23 (2003) 1298
7. T.E. Friedmann, C. Barborka, *J. Biol. Chem.* 141 (1941) 993
8. H. Haljamae, *Intens. Care World* 4 (1987) 118
9. G.A. Brooks, *Fed. Proc.* 45 (1987) 2924
10. Y.B. Hu, G.S. Wilson, *J. Neurochem.* 69 (1997) 1484
11. M.G. Larrabee, *J. Neurochem.* 64 (1995) 1734
12. C.L. Poitry–Yamate, S. Poitry, M. Tsacopoulos, *J. Neurosci.* 15 (1995) 5179
13. A. Schurr, J.J. Miller, R.S. Payne, B.M. Rigor, *J. Neurosci.* 19 (1999) 34
14. L. Pellerin, P,J. Magistretti, *Proc. Nat. Acad. Sci. USA* 91(1994) 10625
15. M. Tsacopoulos, P.J. Magistretti, *J. Neurosci.* 16 (1996) 877
16. A.K. Bouzier–Sore, P. Voisin, V. Bouchaud, E. Bezancon, J.M. Franconi, L. Pellerin, *Euro. J. Neurosci.* 24 (2006) 1687
17. Y. Itoh, T. Esaki, K. Shimoji, M. Cook, M.J. Law, E. Kaufman, L. Sokoloff, *Proc. Natl. Acad. Sci. USA* 100 (2003) 4879
18. L. Pellerin, G. Pellegri, P.G. Bittar, Y. Charnay, C. Bouras, J.L. Martin, N. Stella, P.J. Magistretti, *Dev. Neurosci.* 20 (1998) 291

19. C.P. Chih, P. Lipton, E.L. Roberts, *Trends Neurosci.* 24 (2001) 573
20. G.A. Dienel, L. Hertz, *J. Neurosci. Res.* 66 (2001) 824
21. J. Korf, *J. Cereb. Blood. Flow Metab.* 26 (2006) 1584.
22. A. Schurr, *J. Cereb. Blood Flow Metab.* 26 (2006) 142
23. D.A. Jones, J. Ros, H. Landolt, M. Fillenz, M.G. Boutelle, *J. Neurochem.* 75 (2000) 1703
24. T. Yao, T. Yano, Y. Nanjyo, H. Nishino, *Anal. Sci.* 19 (2003) 61
25. Y. Dong, L. Wang, D. Shangguan, X. Yu, R. Zhao, H. Han, G. Liu, *Neurochem. Int.* 43 (2003) 67
26. R.D. O'Neill, G. Rocchitta, C.P. McMahon, P.A. Serra, J.P. Lowry, T*rends Anal. Chem.* 27 (2008) 78
27. J.B. Gramsbergen, J. Skjøth–Rasmussen, C. Rasmussen, K.L. Lambertsen, *J. Neurosci. Meth.* 140 (2004) 93
28. T. Yao, G. Okano, *Anal. Sci.* 24 (2008) 1469
29. M.C Parkin., S.E. Hopwood, D.A. Jones, P. Hashemi, H. Landolt, M. Fabricius, M. Lauritzen, M.G. Boutelle, A.J. Strong, *J. Cereb. Blood Flow Metab.* 25 (2005) 402
30. R.D. O'Neill, J.L. Gonzalez–Mora, M.G. Boutelle, D.E. Ormonde, J.P. Lowry, A. Duff, B. Fumero, M. Fillenz, M. Mas, *J. Neurochem.* 57 (1991) 22
31. R.D. O'Neill, J.P. Lowry, M. Mas, *Crit. Rev. Neurobiol.* 12 (1998) 69
32. P. Salazar, M. Martín, R. Roche, R.D. O'Neill, J.L. González–Mora, *Electrochim. Acta* 55 (2010) 6476
33. P. Salazar, M. Martín, R. Roche, J.L. González–Mora, R.D. O'Neill, *Biosens. Bioelectron.* 26 (2010) 748
34. P. Salazar, R.D. O'Neill, M. Martín, R. Roche, J.L. González–Mora, *Sensors Act. B–Chem.* 152 (2011) 137
35. R. Roche, P. Salazar, M. Martín, F. Marcano, J.L. González–Mora, J. *Neurosci. Meth.* 202 (2011) 192
36. G. Paxinos, C. Watson, *The Rat Brain in Stereotaxic Coordinates*, Academic Press, Sydney (1986)
37. F. Ricci, G. Palleschi, *Biosens. Bioelectron.* 21 (2005) 389
38. K. Itaya, N. Shoji, I. Uchida, J. *Am. Chem. Soc.* 106 (1984) 3423
39. J.J. García–Jareño, J.J. Navarro, A.F. Roig, H. Scholl, F. Vicente, *Electrochim. Acta* 40 (1995) 1113
40. A. Goux, J. Ghanbaja. A. Walcarius, *J. Mater. Sci.* 44 (2009) 6601
41. M. Zhou, L. Shang, B. Li, L. Huang, S.J. *Dong, Biosens. Bioelectron.* 24 (2008) 442
42. Y. Liu, X. Qu, H. Guo, H. Chen, B. Liu, S. Dong, *Biosens. Bioelectron.* 21 (2006) 2195
43. I.L. Mattos, L. Gorton, T. Laurell, A. Malinauskas, A.A. Karyakin, *Talanta* 52 (2000) 791
44. I.L. Mattos, L. Gorton, T. Ruzgas, *Biosens. Bioelectron.* 18 (2003) 193
45. J.D. Qiu, H.Z. Peng, R.P. Liang, J. Li, X.H. Xia, *Langmuir* 23 (2007) 2133
46. P.J. Kulesza, S. Zamponi, M.A. Malik, K. Miecznikowski, M. Berrettoni, R. Marassi, *J. Solid State Electrochem.* 1 (1997) 88
47. S.A. Agnihotry, P. Singh, A. G. Joshi, D.P. Singh, K.N. Sood, S.M. Shivaprasad, *Electrochim. Acta* 51 (2006) 4291
48. J.D. Breccia, M.M. Andersson, R. Hatti–Kaul, *Biochim. Biophys. Acta* 1570 (2002) 165
49. S.A. Rothwell, S.J. Killoran. R.D. O'Neill, *Sensors* 10 (2010) 6439
50. S.S. El Atrash, R.D. O'Neill, *Electrochim. Acta* 40 (1995) 2791
51. M. Demestre, M. Boutelle, M. Fillenz, *J. Physiol.* 499 (1997) 825
52. N.F. Shram, L.I. Netchiporouk, C. Martelet, N. Jaffrezic–Renault, C. Bonnet, R. Cespuglio, *Anal. Chem.* 70 (1998) 2618
53. R.D. O'Neill, *Analyst* 118 (1993) 433
54. R. Garjonnyte, Y. Yigzaw, R. Meskys, A. Malinauskas, L. Gorton, *Sensors Act. B–Chem.* 79 (2001) 33
55. N.G. Patel, A. Erlenkötter, K. Cammann, G.–C. Chemnitius, *Sensors Act. B–Chem.* 67 (2000)134

56. A. Ges, F. Baudenbache, *Biosens. Bioelectron.* 26 (2010) 828
57. J. Haccoun, B. Piro, V. Noël, M.C. Pham, *Bioelectrochemistry* 68 (2006) 218
58. L. Cheng–Li, S. Cheng–Ling, C. Lai–Kwan, *Anal. Chem.* 79 (2007) 3757
59. A. Poscia, D. Messeri, D. Moscone, F. Ricci, F. Valgimigli, *Biosens. Bioelectron.* 20 (2005) 2244
60. S.A.M. Marzouk, V.V. Cosofret, R.P. Buck, H. Yang, W.E. Cascio, S.S.M. Hassan, Talanta 44 (1997) 1527
61. N. Shram, L. Netchiporouk, R. Cespuglio, *Eur. J. Neurosci.* 16 (2002) 461
62. J.J. Burmeister, M. Palmer, G.A. Gerhardt, *Biosens. Bioelectron.* 20 (2005) 1772
63. J.C Goodman, A.B Valadka, S.P.Gopinath, M. Cormio, C.S. Robertson, *J. Neurotrauma* 13 (1996)549
64. M.L. Hitchman, *Measurement of dissolved oxygen*; John Wiley, New York (1978)
65. F.B. Bolger, J.P. Lowry, *Sensors* 5 (2005) 473